Enantioselective Hydrogenation of Alkenes with Iridium–PHOX Catalysts: A Kinetic Study of Anion Effects

Sebastian P. Smidt,[a] Nicole Zimmermann,[a] Martin Studer,[b] and Andreas Pfaltz*[a]

Abstract: In the asymmetric hydrogenation of unfunctionalized olefins with cationic iridium–PHOX catalysts, the reaction kinetics and, as a consequence, catalyst activity and productivity depend heavily on the counterion. A strong decrease in the reaction rate is observed in the series $[Al\{OC(CF_3)_3\}_4]^- > BAr_F^- > [B(C_6F_5)_4]^- > PF_6^- \gg BF_4^- > CF_3SO_3^-$. With the first two anions, high rates, turnover frequencies (TOF > 5000 h^{-1} at 4 °C), and turnover numbers (TONs) of 2000–5000 are routinely achieved. The hexafluorophosphate salt reacts with lower rates, although they are still respectable; however, this salt suffers from deactivation during the reaction and extreme water-sensitivity, especially at low catalyst loading. Triflate and tetrafluoroborate almost completely inhibit the catalyst. In contrast to the hexafluorophosphate salt, catalysts with $[Al\{OC(CF_3)_3\}_4]^-$, BAr_F^-, and $[B(C_6F_5)_4]^-$ as counterions do not lose activity during the reaction and remain active, even after all the substrate has been consumed. In addition they are much less sensitive to moisture and, in general, rigorous exclusion of water and oxygen is not necessary. A first-order rate dependence on the hydrogen pressure was determined for the BAr_F^- and the PF_6^- salts. At low catalyst loading, the rate dependence on catalyst concentration was also first order. The rate dependence on the alkene concentration was strikingly different for the two salts. While the reaction rate observed for the BAr_F^- salt slightly decreased with increasing alkene concentration (rate order −0.2), a rate order of ≈1 was determined for the corresponding hexafluorophosphate at low alkene concentrations.

Keywords: asymmetric hydrogenation · iridium · kinetics · N,P ligands · oxazolines

Introduction

Enantioselective hydrogenation of olefins with chiral rhodium or ruthenium catalysts has reached a very high level of development.[1] Nevertheless, there are still many classes of substrates that give unsatisfactory results with these catalysts. Unfunctionalized olefins are particularly difficult substrates because, in general, a polar group adjacent to the C=C bond, which coordinates with the metal center, is required for high catalyst activity and enantioselectivity. There are only few examples of highly enantioselective hydrogenations of olefins devoid of a coordinating group.[2,3,4] We have recently found a new class of catalysts, namely, iridium complexes with chiral P,N ligands, which overcome these limitations.[5] These catalysts showed exceptionally high activity with unfunctionalized olefins and, in many cases, they reacted with excellent enantioselectivity. In addition, promising results were also obtained for certain functionalized alkenes for which no suitable catalysts were available. In terms of reactivity, Ir–phosphinooxazoline (PHOX) complexes[5a] resemble the Crabtree catalyst,[6] an achiral cationic (phosphine)(pyridine)Ir complex.

There is little known about the nature of the catalytically active species and the mechanism of hydrogenation with these iridium catalysts. Shortly after completion of the work described herein, a computational study together with some kinetic data of Ir–PHOX catalysts was published by Brandt et al.[7] A catalytic cycle that proceeded via iridium(III) and iridium(V) species was proposed, based on DFT calculations and the observed first-order rate dependence on the hydrogen pressure and the zeroth-order dependence on the substrate concentration. Although such a mechanism is compatible with the kinetic data, the experimental facts accumulated so far do not exclude a more conventional Ir^I–Ir^{III} cycle.

The counterion of the cationic Ir complex plays a crucial role in the catalytic process.[5] Coordinating anions, such as

[a] Dr. S. P. Smidt, Dr. N. Zimmermann, Prof. Dr. A. Pfaltz
Department of Chemistry, University of Basel
St. Johanns-Ring 19, 4056 Basel (Switzerland)
Fax: (+41) 61-267-1103
E-mail: andreas.pfaltz@unibas.ch

[b] Dr. M. Studer
Solvias AG, 4002 Basel (Switzerland)

Supporting information for this article is available on the WWW under http://www.chemeurj.org/ or from the author. The information includes drawings of the experimental set-up for the reactions, additional tables, and other representations for the X-ray crystal structure of **3f**.

 DOI: 10.1002/chem.200400284

halides, and even the weakly coordinating triflate almost completely deactivate the catalyst. The hexafluorophosphate salt exhibits a high reactivity with fast initial rates; however, at low catalyst loadings, it suffers from deactivation before the reaction is complete. Surprisingly, the bulky lipophilic tetraarylborate anion BAr_F^- (tetrakis(3,5-bis-trifluoromethyl-phenyl)borate)[8] strongly enhances the lifetime of the catalyst so that high rates and full conversion can be achieved at low catalysts loadings. Herein we report the results of a kinetic study of Ir–PHOX catalysts with different anions that clearly show how the anion influences the reactivity and stability of the catalyst.

Results and Discussion

Initial studies with the [Ir(PHOX)]BAr_F catalyst 3d: The hydrogenation of (*E*)-1,2-diphenyl-1-propene (**1**) was chosen as the standard reaction for our studies (Scheme 1). All reactions were set up under inert conditions. Five minutes after pressurizing the autoclave with hydrogen gas, the reaction was started by turning on the stirrer. The reaction mixture in the autoclave was kept at a constant hydrogen pressure, and the progress of the reaction was monitored by measuring the pressure drop in a high-pressure reservoir that supplied hydrogen to the autoclave. The maximum reaction rate, v_{max} [mol $L^{-1}h^{-1}$], and conversion were determined from the hydrogen consumption curve. The conversion was determined independently by GC and the enantiomeric excess (*ee*) by HPLC on a chiral column at the end of the reaction. No samples were taken during the reaction because this would have influenced the rate measurements.

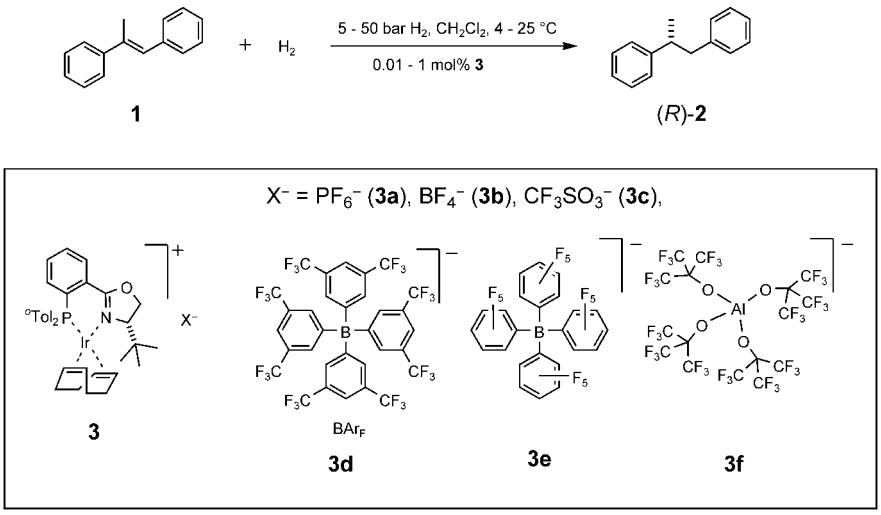

Scheme 1.

Typical hydrogen consumption curves for the hydrogenation of substrate **1** at 4 and 25 °C with the [Ir(PHOX)]BAr_F catalyst **3d** are shown in Figure 1. An induction period is observed in the initial phase of the reaction. During the first minutes, the curve is dominated by gas transfer to the liquid phase induced by stirring. In the subsequent, more important part of the induction period, the active catalyst is generated by hydrogenation and concomitant dissociation of 1,5-cyclooctadiene (cod). Sometimes, especially for low catalyst concentrations, a relatively long induction period was observed. From rhodium-catalyzed hydrogenation it is known that catalyst activation by cod hydrogenation may take a considerable amount of time.[9] The induction period is followed by a relatively long linear section of the curve that indicates constant hydrogen consumption. Maximum rates were taken from this linear section. However, for reactions with long induction periods, the choice of the reaction section with the maximum rate was not always unambiguous. Therefore, the data should be interpreted with caution.

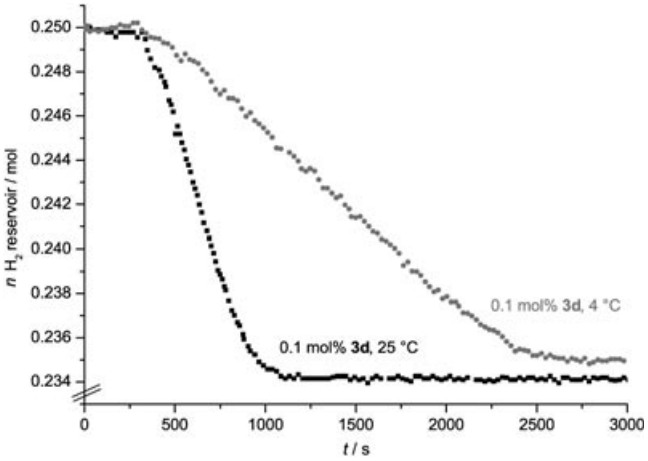

Figure 1. Hydrogen consumption curves for **3d** at two temperatures and 14 bar H_2.

Data from reactions with different catalyst loadings showed a nonlinear relationship between rate and catalyst concentration, with decreasing turnover frequencies (TOFs) at higher catalyst loadings. This confirmed earlier findings[5b] that the reaction at 25 °C is gas–liquid mass-transfer limited, even at low catalyst loadings of 0.1 mol %. Therefore, subsequent experiments were all performed at 4 °C to reduce the reaction rate. With 0.1 mol % catalyst at 4 °C, the reaction time was prolonged to 45 min for full conversion compared to 15 min at 25 °C. In addition, a longer induction period was observed at low temperatures (Figure 1).

The experimental set-up, purification procedures, and handling of the reaction components strongly influence the reproducibility of the rate measurements. Earlier experiments at 25 °C with catalyst **3d** could be reproduced with deviations of the maximum reaction rates below 7 %. At

4 °C, the rates were about two times faster than those determined previously. A possible explanation for this difference could be the deactivating effect of water (vide infra) or other impurities. Even with the utmost care taken to exclude moisture and air, the content of residual water in the reaction mixture cannot always be kept at the same level. However, within the same series of experiments that used the same catalyst, substrate, and solvent batches, the results were reproducible.

Comparison of catalysts with different anions: To study the influence of the counterion, BAr_F^-[8] and PF_6^- salts (**3d**, **3a**) were compared to the corresponding $[B(C_6F_5)_4]^-$, $CF_3SO_3^-$, $[Al\{OC(CF_3)_3\}_4]^-$,[10] and BF_4^- salts (**3e**, **3c**, **3f**, and **3b**, respectively). The aluminate salt **3f** was synthesized from the iridium(cod)chloro dimer, PHOX ligand, and the air- and water-stable lithium aluminate $Li[Al\{OC(CF_3)_3\}_4]$[10c,11] following standard procedures. Complex **3f** was crystallized and characterized by single-crystal X-ray diffraction (Table 1 and Figure 2). The overlay of the cations in **3f** and **3a** showed no significant differences. The smallest distances between anion and cation are measured from the *ortho*-tolyl group (242 pm between F and methyl, 254 pm between F and the *para*-H). Closest contacts between PF_6^- and the cation in **3a** are of similar order: 246 pm between the oxazoline-CH_2 and F, 251 pm between *o*-Tol-CH_3 and F, and 253 pm between *t*Bu and F.

Table 1. Selected bond lengths [pm] and angles [°] in **3f**. For the cation, values for both independent moieties in the unit cells are given with the crystallographic esd's. The values for the anion are averaged over all bonds with standard deviations given in parentheses.

Ir–P	Ir–N	Al–O	O–C(CF_3)$_3$	C–F
229.2(1)	210.2(3)	171.0(8)	134.3(10)	132.3(5)
228.55(13)	209.3(4)			
P-Ir-N		O-Al-O		
85.15(9)		109.5(2)		
85.99(14)				

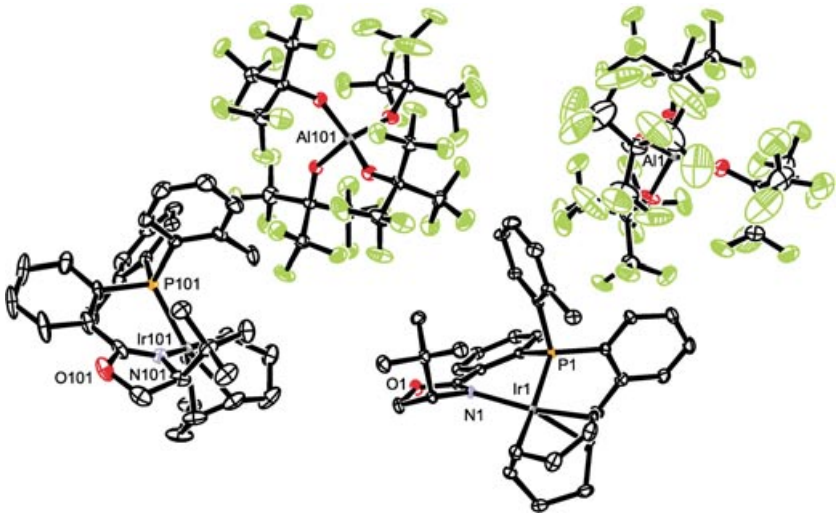

Figure 2. Single-crystal X-ray structure of **3f** with two molecules per unit cell. Ellipsoids drawn at 30 % probability level with Ortep-3 for Windows.[21]

The catalytic activity of complexes **3a–f** was compared under standard conditions at 4 °C, 14 bar H_2, and 0.1 mol % catalyst loading (Table 2 and Figure 3). Complex **3f**, containing the aluminate anion, $[Al\{OC(CF_3)_3\}_4]^-$, is the most active catalyst found so far: $v_{max} = 1.86\,mol\,L^{-1}h^{-1}$ corresponding to a maximum turnover frequency (TOF_{max}) of 5059 h^{-1}, which is approximately 10 % faster than the rate observed with the corresponding BAr_F^- salt **3d** and the same catalyst loading. The rate induced by catalyst **3e** with the perfluorinated tetraphenylborate is 17 % slower than that with **3d**. In summary, the three complexes **3d**, **3e**, and **3f** are the most efficient catalysts and give full conversion with very high TOFs.

Table 2. Hydrogenation with 0.1 mol % catalyst salts **3** with six different anions.[a]

Catalyst	v_{max} [mol L^{-1} h^{-1}]	GC conversion [%]	*ee* [%] (*R*)
3a	0.63	52	97.3
3b	0.12	13	97.9
3c	0	0	n.d.
3d	1.70	> 99	96.9
3e	1.42	> 99	97.2
3f	1.86	> 99	97.3

[a] Reaction conditions: 2.5 g (12.896 mmol) **1**, CH_2Cl_2 (35 mL), 4 °C, stirring at 1200 min^{-1}, 14 bar H_2.

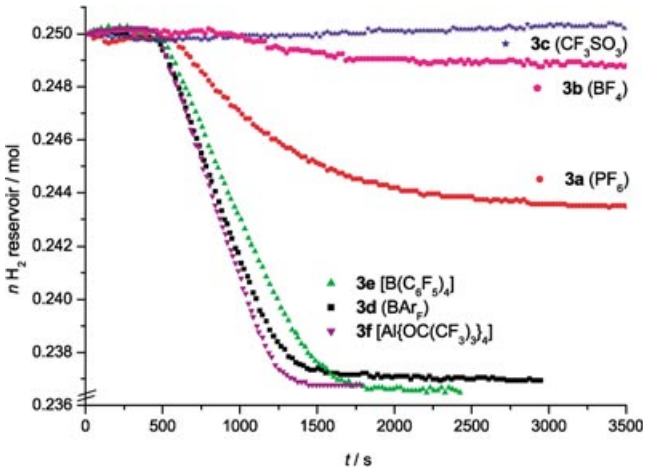

Figure 3. Hydrogen consumption for catalytic reactions with 0.1 mol % of **3** with six different anions at 14 bar H_2, 4 °C, stirring speed 1200 min^{-1}.

For the triflate salt **3c**, no conversion was observed based on the hydrogen consumption and GC analysis of the reaction mixture. At 50 bar and 1 mol % catalyst, traces of product were formed; howev-

er, conversion was less than 1%. The lack of reactivity is probably caused by coordination of the triflate anion to the cationic iridium center.[12] The tetrafluoroborate salt **3b** is slightly more active, but only 13% conversion was observed after 60 min at 14 bar H_2 and 4°C. At 50 bar and room temperature with 1 mol% catalyst, 70% conversion was obtained. In summary, the catalytic activity of complexes **3a–f** strongly depends on the anion and increases in the order $CF_3SO_3^- < BF_4^- \ll PF_6^- < [B(C_6F_5)_4]^- < BAr_F^- < [Al\{OC(CF_3)_3\}_4]^-$.

To check the activity of the catalyst after hydrogen uptake had ceased, an additional 50% of the substrate was added after release of the hydrogen pressure and purging the autoclave with argon (see Table in the Supporting Information). A remarkable difference between the PF_6^- and BAr_F^- salts (**3a**, **3d**) was observed: whereas the PF_6^- salt had completely lost its activity, full conversion of the added substrate was observed with the BAr_F^- salt. The maximum rate was 0.32 mol L^{-1} h^{-1} or 24% of the value obtained for the first batch. This demonstrates that a significant part of the catalyst must still be active after full conversion. Complexes **3e** and **3f** showed essentially the same behavior as the BAr_F^- salt.

To examine the influence of a chiral anion, iridium-PHOX complexes **5a** and **5b** with *Δ*-TRISPHAT[13] were prepared (Scheme 2). Catalyst **5a**, derived from the achiral

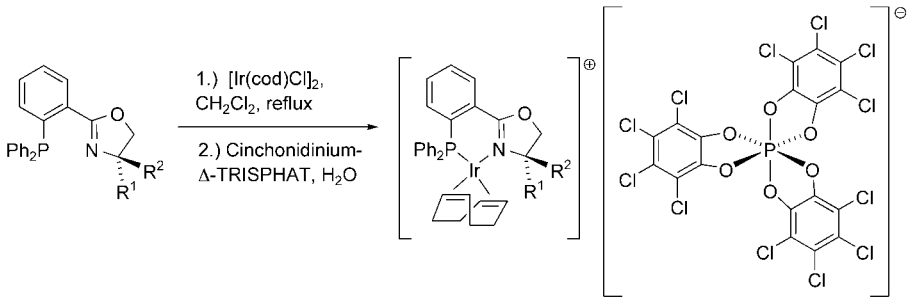

4a: $R^1 = R^2 = CH_3$
4b: $R^1 = i$Pr, R^2 = H, (*S*)

5a: 78%
5b: 83%

Scheme 2.

PHOX ligand **4a**, produced a racemic product in the hydrogenation of the standard substrate **1**. Complex **5b**, derived from the chiral PHOX ligand **4b**, induced the same enantiomeric excess as the corresponding BAr_F^- salt. From these findings we conclude that the anion is quite remote from the coordination sphere of the iridium complex during the enantioselective step, otherwise the chiral anion should exhibit at least a small effect.

Solvent effects: The best solvent was found to be dichloromethane. More strongly coordinating solvents deactivate the catalyst. 1,2-Dichloroethane and toluene can be used as well with similar activities. Hydrogenation of the standard substrate **1** with 0.1 mol% **3d** in 1,2-dichloroethane proceeded with 38% of the maximum rate observed in dichloromethane (Figure 4). Nevertheless, full conversion was achieved at 14 bar. On the other hand, the performance of the

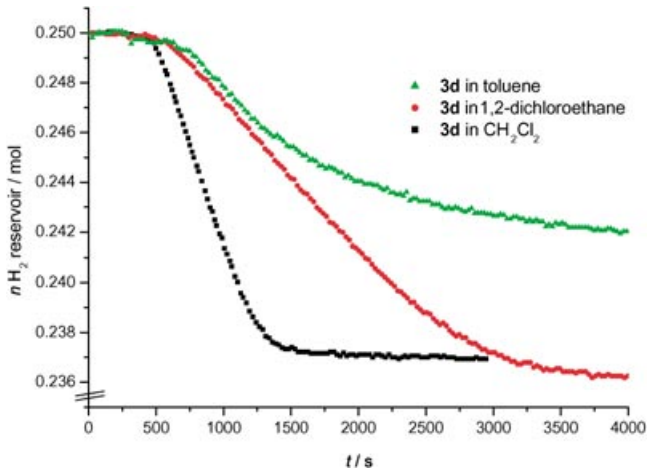

Figure 4. Solvent effects for catalyst **3d**.

PF_6^- salt **3a** is better in 1,2-dichloroethane than in dichloromethane. With 0.1 mol% of **3a** in 1,2-dichloroethane, the maximum reaction rate was 18% lower than in dichloromethane; however, the conversion increased from 52% to 82%.

Only 75% conversion was obtained in small-scale experiments with 0.1 mmol of substrate and 0.1 mol% catalyst **3d** in toluene at 50 bar H_2 after 2 h. Although at a catalyst loading of 0.1 mol%, the solubility of the $[Ir(PHOX)(cod)]^+$ precursor is not a problem, a significant amount of iridium hydrido species precipitated as a viscous yellow oil during the reaction. It is possible that, after dissociation of the cod, the complex becomes less soluble and, therefore, is partially removed from the reaction solution. Preliminary experiments indicate that iridium catalysts with more lipophilic phosphinite ligands, which enhance the solubility,[5f] are more active in toluene.

Kinetic measurements were performed in toluene and compared to analogous data obtained in dichloromethane. The reactions were considerably slower and were stopped after 75 min (**3d**) and 80 min (**3e**), respectively, when the catalysts were probably still active. Catalyst **3d** gave 67% conversion, but the maximum rate (0.59 mol L^{-1} h^{-1}) was only one third of the rate in dichloromethane. With complex **3e**, only about 1/3 of the substrate was hydrogenated with 22% of the maximum rate in CH_2Cl_2.

Effect of water: Preliminary studies had shown that small amounts of water can strongly deactivate the catalyst. Therefore, the effect of water on the kinetics of hydrogenation with 0.1 mol% of catalysts **3a**, **3d**, **3e**, and **3f** was studied (Table 3). The reaction rate with **3d** is decreased by 21% upon addition of 0.05% (v/v) water, but it still gives full conversion. Complex **3a**, on the other hand, is almost

Table 3. Effect of water content.[a]

Catalyst	Water [%] (v/v)	v_{max} [mol L^{-1} h^{-1}]	Decrease in v_{max}	GC conv. [%]
3a	0	0.63		>99
3a	0.05	<0.1	>86%	5
3d	0	1.70		>99
3d	0.05	1.35	21%	>99
3e	0	1.42		>99
3e	0.05	1.34	6%	>99
3f	0	1.86		>99
3f	0.05	1.18	37%	>99

[a] Reaction conditions: **1** (0.368 mol L^{-1}) in dry CH_2Cl_2, 0.1 mol% **3**, reactions set up under argon, with and without addition of degassed water, 4°C, 14 bar H_2, stirring at 1200 min^{-1}.

completely deactivated by the same amount of added water, as seen by the strong decrease of conversion from >99% to 5%. This dramatic effect caused by small amounts of water possibly explains why the performance of the PF_6^- salt (**3a**) at low catalyst loadings is critically dependent on the solvent quality and reaction setup.[14]

The $[B(C_6F_5)_4]^-$ salt **3e** is the least water-sensitive catalyst, showing only a 6% rate decrease after addition of 0.05% (v/v) water. While the $[Al\{OC(CF_3)_3\}_4]^-$ salt **3f** is the most active catalyst under strictly anhydrous conditions, it is strongly affected by the addition of water, resulting in a rate decrease of 37% in the presence of 0.05% (v/v) water. However, the reaction rate still remains at a respectable level of 1.18 mol L^{-1} h^{-1}. The three catalysts **3d**, **3e**, and **3f** all give full conversion in the presence of 0.05% (v/v) water. Thus, at the expense of a modest rate decrease, small amounts of water in the reaction medium can be tolerated.

The extreme water-sensitivity of the PF_6^- salt **3a** could explain why conversions were significantly lower in earlier studies[5b] than the values reported here. In these early experiments, hydrogen gas from a central supply system of poorly defined quality was used. With high-purity hydrogen gas (99.995%) under strictly anhydrous conditions, full conversion was routinely achieved with catalyst loadings as low as 0.4 mol%. We attribute these remarkable differences to the sensitivity of the catalytic system towards water that stems either from the solvent, the catalyst, the substrate, or the hydrogen gas.

Variation of catalyst loading: Complex **3d** is a highly active catalyst giving full conversion at loadings as low as 0.02 mol% at room temperature. At 4°C, more catalyst is necessary to achieve full conversion. With less than 0.05 mol% at 4°C, irreversible deactivation of the catalyst takes place before the reaction reaches completion (86% conversion with 0.025 mol%, 13% conversion with 0.01 mol%). To obtain full conversion with **3a**, at least 0.4 mol% catalyst is necessary. As mentioned above, complex **3a** is highly sensitive to water and, therefore, full conversion is only observed under strictly anhydrous conditions. Otherwise, deactivation of the catalyst becomes a problem, even at loadings of 2–4 mol%.

Hydrogen consumption curves for different concentrations of catalyst **3a** are shown in Figure 5. Analogous data

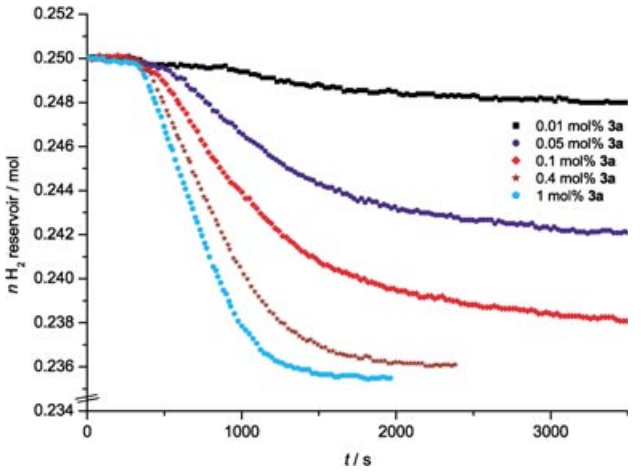

Figure 5. Hydrogen consumption at 4°C, 0.01 to 1 mol% **3a** (PF_6),[**1**]$_0$ = 0.368 mol L^{-1}, 14 bar H_2.

was obtained from complex **3d**. At low catalyst loadings (0.01–0.1 mol%), the rate order with respect to catalyst is ≈1 (0.9 for **3a**, 1.1 for **3d**). At high catalyst loadings, the reaction order strongly decreases for both catalysts (Figure 6).

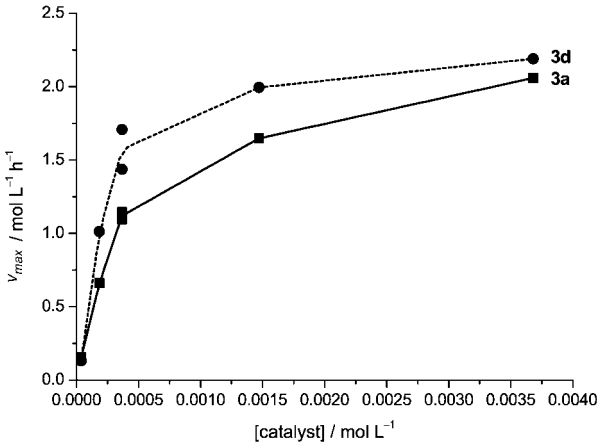

Figure 6. Plot of the dependence of the maximum reaction rate on [catalyst] for **3a** and **3d**. Data points correspond to 0.01, 0.05, 0.1, 0.4, and 1 mol% loading. All at 4°C,[**1**]$_0$ = 0.368 mol L^{-1}, 14 bar H_2.

This could be caused by gas–liquid mass-transfer limitation at higher catalyst loadings or concentration-dependent deactivation, for example, by formation of unreactive trimeric hydride-bridged complexes.[15]

Table 4 lists the TOF_{max} for different catalyst concentrations. The TOF_{max} values decrease from 4200 to 560 h^{-1}

Table 4. Turnover frequencies (TOF) for different concentrations of **3a** and **3d** at 4°C

mol% **3**	**3a** TOF_{max} [h^{-1}]	**3a** GC conv. [%]	**3a** *ee* [%], (*R*)	**3d** TOF_{max} [h^{-1}]	**3d** GC conv. [%]	**3d** *ee* [%], (*R*)
0.01	**4236**	13	97.2	3588	3	n.d.
0.05	3600	58	98.0	**5502**	94	96.2
0.1	2976	78	97.4	4632	>99	96.6
0.4	1122	99	97.9	1338	>99	97.3
1	558	>99	98.0	59	>99	97.5

when the catalyst concentration is increased from 0.01 to 1 mol% for **3a** and from 5500 to 60 h^{-1} between 0.05 and 1 mol% for $[\mathbf{3d}]_0$. The highest TOF_{max} was obtained for 0.05 mol% **3d**, thus giving a TOF_{max} of 5500 h^{-1} with BAr_F^- as the counterion at 4°C. Catalysts **3e** and **3f** gave similar results (see Supporting Information).

In one experiment with **3d**, seven samples were taken during the course of the reaction to see whether the *ee* changes with conversion. As shown in Table 5, the *ee* remains constant within experimental error throughout the reaction.

Table 5. Change of *ee* values during the catalytic reaction with 0.1 mol% **3d** at 14 bar H_2 and 4°C.

GC conversion [%]	9	18	26	35	43	54	84	average
ee [%], (*R*)	98.0	98.0	98.3	98.0	98.0	97.9	98.1	98.0±0.1

Variation of alkene concentration: The alkene concentration was varied from 73.5 mmol L^{-1}, which is the lowest value from which reliable data could be obtained, to 735 mmol L^{-1}, while the catalyst concentration was kept constant at 368 μmol L^{-1}. With **3d**, a slight decrease in the reaction rate was observed as the alkene concentration was increased. A logarithmic plot of the data shown in Figure 7

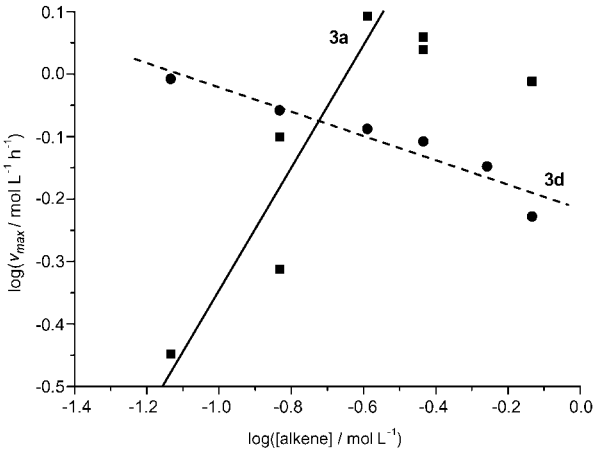

Figure 7. Double logarithmic plot of the dependence of the maximum reaction rate on the alkene concentration for **3a** and **3d** (0.1 mol% each, 4°C, 14 bar H_2). The data points correspond to $[\mathbf{1}]_0$ = 0.074, 0.147, 0.257, 0.368, 0.552, and 0.736 mol L^{-1}. Linear fit for **3a**: $y = 0.64 + 0.98x$ (R^2 = 0.85, σ = 0.11), linear fit for **3d**: $y = -0.22 - 0.19x$ (R^2 = 0.91, σ = 0.026).

yields a reaction order of −0.2 based on the alkene concentration. This weak negative effect could be caused by impurities in the alkene, which deactivate the catalyst. Because the impurities increase proportionally to the alkene concentration, while the amount of catalyst remains the same, the catalytic activity decreases at higher alkene concentrations. Changes in the solvent parameters, such as polarity resulting from the higher alkene concentration, could also affect the reaction rates. However, because of the difficulties in determining exact maximum rates (vide supra), the data should be interpreted with caution. Nevertheless, the observed reaction order, which is close to zero, implies that the alkene is not involved in the rate-limiting step. Furthermore, there is no significant influence of the alkene concentration on the enantioselectivity.

Catalyst **3a** shows a strikingly different behavior: a double logarithmic plot reveals a rate order of ≈1 for alkene concentrations between 0.074 and 0.26 mol L^{-1}. However, the pronounced induction periods observed in these reactions lead to relatively large errors in the maximum rates, which prevent a detailed analysis of the data. The reason for the low rate at 0.74 mol L^{-1} is unclear. Additional measurements in the concentration range above 0.3 mol L^{-1} will be necessary to reveal the rate dependence at high alkene concentrations. Nevertheless, the data obtained at low alkene concentration clearly show that the anion has a strong effect on the reaction kinetics.

A possible origin of the striking difference between the BAr_F^- and the PF_6^- salt could be the stronger coordination of the hexafluorophosphate ion. Coordination of the PF_6^- ion could either shift the equilibrium from an alkene complex toward a hexafluorophosphate complex or slow down the addition of the alkene to the iridium center to such an extent that it becomes rate-limiting. In contrast, the very weakly coordinating BAr_F^- ion does not interfere with alkene coordination and, therefore, the catalyst is saturated with alkene, even at low alkene concentrations. This interpretation could also explain the much higher tendency of the PF_6^- salt to deactivate during the reaction. We found that deactivation is accompanied by formation of an inactive hydride-bridged trimeric iridium complex.[15] If this trimerization is responsible for the observed deactivation, then the critical step in the catalytic cycle is the reaction of an iridium hydride intermediate with the alkene, which competes with trimerization. The reaction with the alkene is faster with the BAr_F^- salt and, as a consequence, the productive hydrogenation pathway dominates over trimerization.

The effects of BAr_F^--containing additives, which were observed in hydrogenations catalyzed by the hexafluorophosphate salt **3a**, are in agreement with this explanation. When a 1 molar equivalent of $[NBu_4][BAr_F]$[16] was added to a solution of **3a** (0.1 mol%; 23°C), conversion increased from 50% to ≈70%. Upon addition of an equimolar amount of $HBAr_F{\cdot}Et_2O$,[16,15b] full conversion was observed and the rate was accelerated by a factor of 1.8. On the other hand, addition of an equimolar amount of $[NBu_4][PF_6]$ to complex **3d** led to a decrease in the conversion from 100 to 80% at 1 mol% catalyst loading. The higher productivity of the hexafluorophosphate salt in the presence of the BAr_F^- ion can be rationalized by partial formation of the more active BAr_F^- salt by anion exchange. These observations and the strikingly different kinetics of the BAr_F^- and the PF_6^- salt are evidence against another possible explanation that partial hydrolysis of the anion, producing strongly coordinating fluoride ions, is responsible for the higher deactivation tendency of the hexafluorophosphate salt.

Variation of hydrogen pressure: The logarithmic plot of maximum reaction rates versus the hydrogen pressure for complex **3d** shows a rate order of 1.0, as expected, if hydro-

gen is involved in the turnover-limiting step (Figure 8). For the hexafluorophosphate salt **3a**, an alkene concentration of 0.147 mol L^{-1} was chosen, which is in the region where the rate order in substrate was found to be unity (see above). In this case, a rate order with respect to hydrogen of approximately 1.5 was found. As noted before, the maximum rate values for the hexafluorophosphate **3a** are significantly less accurate than for the BAr_F^- salt **3a**. Therefore, it cannot be excluded that deviation from a first-order rate dependence is caused by artifacts resulting from the pronounced induction periods in these reactions. Nevertheless, the data for both catalysts **3a** and **3d** clearly show that hydrogen is involved in the rate-limiting step.

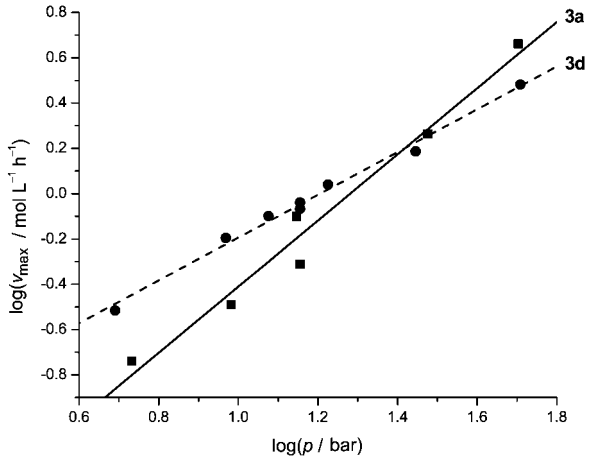

Figure 8. Influence of the hydrogen pressure (5–50 bar H_2, 4 °C). Conditions: CH_2Cl_2, 4 °C; a) 0.1 mol % **3a**, $[\mathbf{1}]_0 = 0.147$ mol L^{-1}; linear fit $y = -1.87 + 1.46x$ ($R^2 = 0.97$, $\sigma = 0.09$); b) 0.1 mol % **3d**, $[\mathbf{1}]_0 = 0.368$ mol L^{-1}; linear fit $y = -1.14 + 0.94x$ ($R^2 = 0.99$, $\sigma = 0.03$).

A small but significant pressure effect on the enantioselectivity in the hydrogenation with catalyst **3d** was found in reactions performed at room temperature (Table 6): if the hydrogen pressure is increased from 5 bar to 96 bar, the *ee* decreases from 97.5 % to 95.4 %. In energetic terms, this corresponds to a difference of 0.4 kcal mol^{-1} for the $\Delta\Delta G^{\neq}$ values.

Table 6. Dependence of the enantioselectivity on hydrogen pressure for catalyst **3d**[17] (CH_2Cl_2, 23 °C).

$p(H_2)$ [bar]	5	10	20	50	96
ee [%], (*R*)	97.5 ± 0.5	97.4 ± 0.3	97.3 ± 0.1	96.2 ± 0.3	95.4 ± 0.3
$\Delta\Delta G^{\neq}$ [kcal mol^{-1}][a]	2.57	2.55	2.52	2.32	2.20

[a] At $T = 296.15$ K.

Conclusion

In the asymmetric hydrogenation of unfunctionalized olefins with cationic iridium–PHOX catalysts, the reaction kinetics and, as a consequence, catalyst activity and productivity heavily depend on the counterion. A strong decrease of the reaction rate is observed in the series $[Al\{OC(CF_3)_3\}_4]^- > BAr_F^- > [B(C_6F_5)_4]^- > PF_6^- \gg BF_4^- > CF_3SO_3^-$. With the first three anions, high rates and TONs of 2000–5000 are routinely achieved. Evidently, extremely weakly coordinating anions are required for this class of catalysts. The hexafluorophosphate salt reacts with lower rates, although they are still respectable. However, the efficiency and practicality of this catalyst are affected by the observed deactivation during the reaction and its extreme water-sensitivity, especially at low catalyst loadings. Triflate and tetrafluoroborate, although they are weak ligands, almost completely inhibit the catalyst. Catalysts with $[Al\{OC(CF_3)_3\}_4]^-$, BAr_F^-, and $[B(C_6F_5)_4]^-$ counterions are not only more reactive but also more stable than the other salts evaluated in this study. In contrast to the hexafluorophosphate salt, they do not lose activity under the usual reaction conditions and remain active even after all the substrate has been consumed. In addition, they are much less sensitive to moisture than the hexafluorophosphate and, in general, rigorous exclusion of water and oxygen is not necessary.

From kinetic data of the BAr_F^- and the PF_6^- salts, an approximately first-order rate dependence on the hydrogen pressure was determined for both complexes. This implies that dihydrogen is involved in the turnover-limiting step. At low catalyst loading, the rate dependence on the catalyst concentration was also first order. These results are consistent with the data reported by Brandt et al.[7] The rate dependence on the alkene concentration was strikingly different for the two salts. While the reaction rate observed for the BAr_F^- salt slightly decreased with increasing alkene concentration (rate order −0.2), a rate order of ≈ 1 was determined for the corresponding hexafluorophosphate at low alkene concentrations. Thus, in the former case, the alkene is not involved in the turnover-limiting step, whereas it is in the latter case. This remarkable anion effect could be the origin of the stability difference between the BAr_F^- and the PF_6^- salt under the reaction conditions. Compared to BAr_F^-, the hexafluorophosphate anion decreases the reaction rate of the alkene with the catalyst, presumably by coordination with the metal center. As a consequence, deactivation leading to an unreactive trimeric hydridoiridium complex competes with the productive hydrogenation pathway. For the BAr_F^- salt, the reaction between the catalyst and the alkene is much faster and, therefore, dominates over the deactivation process.

In summary, our kinetic data show that iridium–PHOX complexes with bulky, very weakly coordinating anions, such as BAr_F^-, $[B(C_6F_5)_4]^-$, or $[Al\{OC(CF_3)_3\}_4]^-$, are highly active and very productive catalysts for the hydrogenation of unfunctionalized olefins. Owing to their low oxygen and water sensitivity, the catalysts can be easily handled under a normal atmosphere and stored at room temperature without decomposition. Further kinetic and mechanistic studies of these catalysts are in progress.

Experimental Section

General: Dichloromethane was freshly distilled from calcium hydride or purchased in sure-seal bottles from Fluka and kept under an inert atmosphere. (*E*)-1,2-Diphenyl-1-propene (**1**) was purchased from Lancaster and used without further purification, or it was prepared from acetophenone and benzylmagnesium chloride.[18] Hydrogen gas used in the experiments was purchased at Carbagas Switzerland (quality 45, 99.995%). Iridium complexes (−)-[(η^4-1,5-cyclooctadiene)-{(4*S*)-2-[(2-(di-*o*-tolylphosphino)phenyl]-4,5-dihydro-4-*tert*-butyl-oxazole}iridium(I)]hexafluorophosphate (**3a**) and (−)-[(η^4–1,5-cyclooctadiene)-{(4*S*)-2-[(2-(di-*o*-tolylphosphino)phenyl]-4,5-dihydro-4-*tert*-butyl-oxazole}iridium(I)]tetrakis[3,5-bis-(trifluoromethyl)phenyl]borate (**3d**) were prepared according to literature procedures.[5a,b] Complexes **3b** and **3c** were prepared from the chloro complex through ion exchange with silver salts. Complex **3e** was prepared from $NaB(C_6F_5)_4$, as for the BAr_F^- complex. $HBAr_F{\cdot}Et_2O$ and $[NBu_4]BAr_F$ were prepared according to literature procedures.[16]

Gas chromatography was carried out on a Carlo Erba HRGC Mega2 Series MFC800 (column: Restek Rtx-1701, 0.25 μm, 30 m, 60 kPa He). HPLC analysis was performed with a Shimadzu SCL-10A with a Daicel Chiralcel OJ column. GC: 21.0 min (**1**), 18.2 min (**2**), (100 °C, 2 min isotherm, 7 °C min^{-1}, 250 °C, 5 min). HPLC: 13.9 min ((*R*)-**2**), 22.7 min ((*S*)-**2**), 27.5 min (**1**), (Chiralcel OJ; 254 nm; heptane/2-propanol 99:1).

(−)-[(η^4-1,5-cyclooctadiene)-{(4*S*)-2-[(2(di-*o*-tolylphosphino)phenyl]-4,5-dihydro-4-*tert*-butyl-oxazole}iridium(I)] tetrakis(perfluoro-*tert*-butoxy)-aluminate (3f): To a stirred solution of (4*S*)-2-[(2(di-*o*-tolylphosphino)-phenyl]-4,5-dihydro-4-*tert*-butyl-oxazole (100 mg, 0.24 mmol) in dry CH_2Cl_2 (5 mL) was added $[\{IrCl(cod)\}_2]$ (81 mg, 0.12 mmol). The red solution was heated for 2 h at 48 °C in a closed vial. After the mixture had been cooled to room temperature, $Li[Al\{OC(CF_3)_3\}_4]$[10] (305 mg, 0.31 mmol) was added, resulting in a lighter color. After 5 min, water (5 mL) was added, resulting in a gel-like mixture. Phase separation was followed by extraction of the organic layer with water and filtration over $MgSO_4$. The light red complex was recrystallized from diethyl ether and pentane to give single crystals suitable for X-ray crystallography (381 mg, 0.23 mmol; 94%).

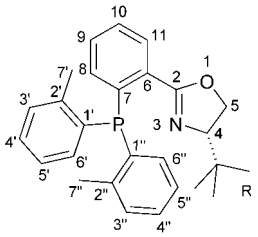

^{1}H NMR (400 MHz, CD_2Cl_2, 300 K, TMS): δ = 0.56 (s, 9H; R), 1.50 (mc, 1H; cod), 1.63 (mc, 1H; cod), 2.08 (mc, 2H; cod), 2.36 (s, 3H; 7′, *o*-Tol_{eq}), 2.44 (mc, 2H; cod), 3.05 (br, 1H; cod *trans* to N), 3.10 (s, 3H; 7″, *o*-Tol_{ax}), 3.48 (br, 1H; cod *trans* to N), 4.00 (br, 1H; cod *trans* to P), 4.41 (dd, ^3J(H,H) = 9.6 Hz, 1H; 4), 4.64 (br d, 1H; 5), 4.79 (dd, ^2J(H,H) = 7.6 Hz, ^3J(H,H) = 9.6 Hz, 1H; 5), 4.93 (mc, 1H; cod *trans* to P), 6.52 (br, 1H; 6″), 6.89 (br d, J(H,H) = 7.1 Hz, 1H; Ar–H), 7.07 (br, 1H; 5″), 7.25 (mc, 3H; Ar–H), 7.44 (mc, 5H; Ar–H), 7.65 (mc, 1H; Ar–H), 7.76 (mc, 1H; Ar–H), 8.30 ppm (d, J(H,H) = 7.9 Hz, 1H; 11); ^{31}P{^{1}H} NMR (163 MHz, CD_2Cl_2, 300 K, $(PhO)_3P{=}O$ δ = 18): two conformers due to hindered rotation around the P–*o*-Tol bond: δ = 9.5 (s, 89%), 17.3 ppm (s, 11%); ^{19}F{^{1}H} NMR (CD_2Cl_2, 376 MHz, 300 K, $FCCl_3$): δ = −76.8 ppm (s); ^{13}C{^{1}H} NMR ($CDCl_3$, 101 MHz; 300 K, TMS): δ = 24.3 (d, ^3J(P,C) = 5.8 Hz; 7″), 24.8 (3 C; *t*Bu-CH_3), 25.2 (cod-CH_2), 25.5 (d, ^3J(P,C) = 4.6 Hz; 7′), 28.2 (cod-CH_2), 32.7 (cod-CH_2), 34.2 (*t*Bu quart. C), 35.5 (cod-CH_2), 67.4 (br; cod-CH *trans* to N), 67.5 (br; cod-CH *trans* to N), 69.9 (5), 74.5 (4), 90.0 (d, ^2J(P,C) = 13.4 Hz; cod-CH *trans* to P), 95.0 (d, ^2J(P,C) = 10.7 Hz; cod-CH *trans* to P), 119.3 (d, ^1J(P,C) = 52.9 Hz, 1′), 121.2 (q, ^1J(F,C) = 292.1 Hz, 12 C; CF_3), 127.1 (5′), 127.2 (5″), 127.9 (6), 128.1 (d, ^1J(P,C) = 61.7 Hz; 7), 130.0 (d, ^1J(P,C) = 45.2 Hz; 1″), 132.3 (4′), 132.4 (4″), 132.7 (3′), 132.7 (3″), 133.2 (8), 133.6 (6″), 133.7 (6′), 134.0 (11), 134.1 (9), 134.7 (10), 141.1 (d, ^2J(P,C) = 8.4 Hz; 2′), 142.9 (d, ^2J(P,C) = 13.4 Hz; 2″), 163.8 ppm (2), 1 quart. C missing (Al-O-*C*$(CF_3)_3$); IR (KBr): $\tilde{\nu}$ = 3067w, 2972m, 2895w, 2848w, 1596m, 1566w, 1489m, 1457m, 1378m, 1353s, 1302vs, 1278vs, 1242vs, 1219vs, 1168s, 1124m, 1070w, 1062w, 974vs, 833m, 756m, 728vs, 684w, 561m, 536m, 511w, 449m cm^{-1}; MS (ESI, CH_2Cl_2): *m*/*z* (%): positive mode: 716.3 ($[M\{^{193}Ir\}-anion)]^+$, 100); negative mode: 967.1 ($[M-cation]^-$, 100); = −93.7 (c = 0.5, $CHCl_3$); elemental analysis calcd (%) for $C_{51}H_{42}AlF_{36}IrNO_5P$: C 36.40, H 2.52, N 0.83; found: C 36.57, H 2.75, N 0.75.

CCDC-201707 contains the supplementary crystallographic data for this paper. These data can be obtained free of charge via www.ccdc.cam.ac.uk/conts/retrieving.html (or from the Cambridge Crystallographic Data Centre, 12 Union Road, Cambridge CB21EZ, UK; fax: (+44) 1223-336033; or deposit@ccdc.cam.uk).

Kinetic studies: The kinetic studies were carried out and interpreted with the isolation as well as the initial rate method.[19] Reactions were carried out in a 50 mL high-pressure autoclave with a magnetic stirrer (typically at 1200 min^{-1}). The vessel was kept at a constant temperature (Haake thermostat) and pressure, and hydrogen was metered through a dosing valve as needed to maintain constant pressure during the reaction. The progress of the reaction was monitored by following the pressure drop in a hydrogen reservoir (33 mL) on the high-pressure side of the dosing valve which was initially set at ≈175 bar. Data pairs of (pressure, time) were collected every 6 s throughout the reaction. The pressure drop was related to the molar uptake of hydrogen using a computer program which was calibrated for this autoclave by Solvias AG. The reaction rate was determined from the maximum slope of the hydrogen pressure drop in the reservoir by means of the computer program ANFGES.EXE. Export of the molar amount of hydrogen in the reservoir was made possible by a small addition to this software.[20] The values obtained were then adjusted by addition of a constant for a starting point of 0.25 mol H_2 in the reservoir to be able to overlay the curves. The conversion was determined by GC analysis, the enantioselectivities were checked by chiral HPLC analysis.

General hydrogenation procedure: The autoclave was purged 4 times with 3–5 bar Ar and cooled to the desired temperature under Ar pressure. (*E*)-1,2-Diphenyl-1-propene and the iridium catalyst were dissolved in dry dichloromethane (35 mL) under argon and transferred versus a counterstream of argon into the autoclave. The autoclave was sealed, purged with argon (3×), and the solution was stirred for 5 min to equilibrate to the temperature. Stirring was stopped, the autoclave was purged with argon (3×) and then with hydrogen (3×, 7–13 bar). After the autoclave had been pressurized to the desired hydrogen pressure, the tightness of apparatus was checked for 5 min by monitoring changes in the reservoir pressure. The reaction was started when stirring was commenced. Stirring was stopped after the reservoir pressure had remained constant for several minutes at the end of the reaction, and the autoclave was depressurized and flushed with Ar (3×). A sample (normally 0.3 mL, depending on the substrate concentration) of the resulting yellow solution was taken and concentrated in vacuo. Heptane (1 mL) was added, and the suspension was filtered through a syringe filter to remove catalyst residues. The resulting solution was used directly for GC and HPLC analysis.

Acknowledgements

We would like to thank Dr. Hans-Ulrich Blaser and Dr. Benoît Pugin (both Solvias AG), Prof. Donna G. Blackmond (Imperial College London), Dr. Lasse Greiner (RWTH Aachen), and Thomas Schultz (University of Basel) for advice and helpful discussions. We also thank Mr. Stephan Burckhardt (formerly Solvias AG) for technical assistance. We are grateful to Dr. Ingo Krossing (University of Karlsruhe) for a sample of $Li[Al\{OC(CF_3)_3\}_4]$ and to Prof. Jérôme Lacour (University of Geneva) for a sample of Δ-TRISPHAT. We thank Mr. Markus Neuburger (University of Basel) for measuring X-ray diffraction data and for his help with the refinement, and Mrs. Esther Hörmann (University of Basel) for valuable experimental contributions. Financial support by the

Swiss National Science Foundation and the Federal Commission for Technology and Innovation (KTI Project No. 5189.2 KTS) is gratefully acknowledged. S.P.S. thanks the Gottlieb Daimler- and Carl Benz-Foundation and the German Academic Exchange Service (DAAD) for Ph. D. fellowships. N.Z. thanks the Fonds der Chemischen Industrie (Frankfurt) and the German Federal Ministry for Science and Technology (BMBF) for a Kekulé Fellowship.

[1] a) J. M. Brown in *Comprehensive Asymmetric Catalysis*, *Vol. I*, Chapt. 5.1 (Eds.: E. N. Jacobsen, A. Pfaltz, H. Yamamoto), Springer, Berlin, **1999**, pp. 121–182; b) R. Noyori, *Angew. Chem.* **2002**, *114*, 2108–2123; *Angew. Chem. Int. Ed.* **2002**, *41*, 2008–2022; c) W. S. Knowles, *Angew. Chem.* **2002**, *114*, 2096–2107; *Angew. Chem. Int. Ed.* **2002**, *41*, 1998–2007.

[2] a) R. D. Broene, S. L. Buchwald, *J. Am. Chem. Soc.* **1993**, *115*, 12569–12570; b) M. V. Troutman, D. H. Appella, S. L. Buchwald, *J. Am. Chem. Soc.* **1999**, *121*, 4916–4917.

[3] a) R. L. Haltermann in *Comprehensive Asymmetric Catalysis*, *Vol. I*, Chapt. 5.2 (Eds.: E. N. Jacobsen, A. Pfaltz, H. Yamamoto), Springer, Berlin, **1999**, pp. 183–195; b) V. P. Conticello, L. Brard, M. A. Giardello, Y. Tsuji, M. Sabat, C. L. Stern, T. J. Marks, *J. Am. Chem. Soc.* **1992**, *114*, 2761–2762.

[4] G. S. Forman, T. Ohkuma, W. P. Hems, R. Noyori, *Tetrahedron Lett.* **2000**, *41*, 9471–9475.

[5] a) A. Lightfoot, P. Schnider, A. Pfaltz, *Angew. Chem.* **1998**, *110*, 3047–3050; *Angew. Chem. Int. Ed.* **1998**, *37*, 2897–2899; b) D. G. Blackmond, A. Lightfoot, A. Pfaltz, T. Rosner, P. Schnider, N. Zimmermann, *Chirality* **2000**, *12*, 442–449; c) J. Blankenstein, A. Pfaltz, *Angew. Chem.* **2001**, *113*, 4577–4579; *Angew. Chem. Int. Ed.* **2001**, *40*, 4445–4447; d) P. G. Cozzi, N. Zimmermann, R. Hilgraf, S. Schaffner, A. Pfaltz, *Adv. Synth. Catal.* **2001**, *343*, 450–454; e) F. Menges, A. Pfaltz, *Adv. Synth. Catal.* **2002**, *344*, 40–44; f) A. Pfaltz, J. Blankenstein, R. Hilgraf, E. Hörmann, S. McIntyre, F. Menges, M. Schönleber, S. P. Smidt, B. Wüstenberg, N. Zimmermann, *Adv. Synth. Catal.* **2003**, *345*, 33–43; g) S. P. Smidt, F. Menges, A. Pfaltz, *Org. Lett.* **2004**, *6*, 2023–2026.

[6] R. Crabtree, *Acc. Chem. Res.* **1979**, *12*, 331–338.

[7] P. Brandt, C. Hedberg, P. G. Andersson, *Chem. Eur. J.* **2003**, *9*, 339–347.

[8] a) H. Nishida, N. Takada, M. Yoshimura, T. Sonoda, H. Kobayashi, *Bull. Chem. Soc. Jpn.* **1984**, *57*, 2600–2604; b) S. R. Bahr, P. Boudjouk, *J. Org. Chem.* **1992**, *57*, 5545–5547; c) M. Brookhart, B. Grant, A. F. Volpe, Jr., *Organometallics* **1992**, *11*, 3920–3922; d) D. L. Reger, T. D. Wright, C. A. Little, J. J. S. Lamba, M. D. Smith, *Inorg. Chem.* **2001**, *40*, 3810–3814.

[9] a) D. Heller, K. Kortus, R. Selke, *Liebigs Ann.* **1995**, 575–581; b) D. Heller, S. Borns, W. Baumann, R. Selke, *Chem. Ber.* **1996**, *129*, 85–89; c) H.-J. Drexler, W. Baumann, A. Spannenberg, C. Fischer, D. Heller, *J. Organomet. Chem.* **2001**, *621*, 89–102; d) C. J. Cobley, I. C. Lennon, R. McCague, J. A. Ramsden, A. Zanotti-Gerosa, *Tetrahedron Lett.* **2001**, *42*, 7481–7483.

[10] a) T. J. Barbarich, Ph.D. Dissertation, Colorado State University, **1999**; b) S. H. Strauss, B. G. Nolan, T. J. Barbarich, J. J. Rockwell, Colorado State University Research Foundation, USA, PCT Int. Appl. No. WO 9912938, **1999**, pp. 47; c) I. Krossing, *Chem. Eur. J.* **2001**, *7*, 490–502; d) S. M. Ivanova, B. G. Nolan, Y. Kobayashi, S. M. Miller, O. P. Anderson, S. H. Strauss, *Chem. Eur. J.* **2001**, *7*, 503–510.

[11] The precursor perfluoro-*tert*-butyl alcohol, if purchased in 100 g amounts from www.apolloscientific.co.uk, costs 4 € per gram or 0.95 € per mmol (I. Krossing).

[12] $CF_3SO_3^-$ can even serve as a ligand in compounds such as $[Cu^I(CF_3SO_3)]_2{\cdot}C_6H_6$: R. G. Salomon, J. K. Kochi, *J. Am. Chem. Soc.* **1973**, *95*, 3300–3310.

[13] J. Lacour, C. Ginglinger, C. Grivet, G. Bernardinelli, *Angew. Chem.* **1997**, *109*, 660–662; *Angew. Chem. Int. Ed. Engl.* **1997**, *36*, 608–610.

[14] P. Schnider, Ph.D. Dissertation, University of Basel, **1996**.

[15] S. P. Smidt, A. Pfaltz, E. Martínez-Viviente, P. S. Pregosin, A. Albinati, *Organometallics* **2003**, *22*, 1000–1009.

[16] R. Taube, S. Wache, *J. Organomet. Chem.* **1992**, *428*, 431–442.

[17] For every data point, between 11 and 20 independent *ee* measurements (integration of HPLC traces) from 4 to 6 independent small-scale reactions (0.1 mmol (**1**), 0.1 mol% (**3d**), RT, 2 h, 0.5 mL CH_2Cl_2) were averaged. The standard deviations given here are from the single *ee* measurements, not from those averaged for each reaction. The error in pressure determination is estimated as follows: 5 ± 0.5 bar, 10 ± 0.5 bar, 20 ± 1 bar, 50 ± 1 bar, 96 ± 2 bar. A linear fit of *ee* versus pressure, including standard deviations, is given in the Supporting Information.

[18] N. Zimmermann, Ph.D. Dissertation, University of Basel, **2001**.

[19] P. W. Atkins, *Physical Chemistry*, 5th ed, Oxford University Press, Oxford, **1995**.

[20] ANFGES.EXE, version 0.99, M. Studer, Solvias AG, **1993**.

[21] L. J. Farrugia, *J. Appl. Crystallogr.* **1997**, *30*, 565.

Received: March 24, 2004
Published online: August 5, 2004

